Revised Tolmachev-Morel-Anderson pseudopotential for layered conventional superconductors with nonlocal Coulomb interaction

M. Simonato, M. I. Katsnelson, and M. Rösner*
Institute for Molecules and Materials, Radboud University, 6525 AJ Nijmegen, the Netherlands

(Received 8 September 2022; revised 9 December 2022; accepted 24 July 2023; published 16 August 2023)

We study the effects of static nonlocal Coulomb interactions in layered conventional superconductors and show that they generically suppress superconductivity and reduce the critical temperature. Although the nonlocal Coulomb interaction leads to a significant structure in the superconducting gap function, we find that most properties can be effectively described by means of an appropriately revised local Coulomb pseudopotential $\tilde{\mu}_C^*$, which is *larger* than the commonly adopted retarded Tolmachev-Morel-Anderson pseudopotential μ_C^*. To understand this, we analyze the Bethe-Salpeter equation describing the screening of Coulomb interaction in the superconducting state and obtain an expression for $\tilde{\mu}_C^*$, which is valid in the presence of nonlocal Coulomb interactions in two dimensions. This analysis also reveals how the structure of the nonlocal Coulomb interaction weakens the screening effects from high-energy pair fluctuations and therefore yields larger values of the pseudopotential. Our findings are especially important for layered conventional superconductors with small Fermi energies and can be readily taken into account within *ab initio* studies.

DOI: 10.1103/PhysRevB.108.064513

I. INTRODUCTION

Conventional superconductivity in the weak and strong electron-phonon coupling limit is well described within Migdal-Eliashberg (ME) theory [1,2], which accurately approximates superconducting properties around the Fermi level [3,4]. When both electron-phonon and electron-electron (Coulomb) interactions are present the corresponding expressions become, however, rather involving [5,6]. Thus, even for the description of conventional superconductivity approximations are required that take the Coulomb repulsion in the pairing channel adequately into account. A conventional scheme to do so was independently introduced by Tolmachev [7] and by Morel and Anderson [8] yielding the famous Tolmachev-Morel-Anderson (TMA) *local* retarded Coulomb pseudopotential μ_C^*. Using appropriate energy scales, the TMA expression provides good estimates for μ_C^* which, together with phonon properties from first principles, yield good agreement with experimental data for many elemental bulk superconductors and their alloys [2,9].

Aside from the successful descriptions obtained with the conventional TMA approach, there are situations in which the details of the Coulomb interaction and its screening become important and need to be carefully considered. This includes the dynamics of the screening, which can lead to plasmonic contributions to superconductivity [10–18] and the possible nonlocal character of the electron-electron interaction. The latter can be crucially important in case of disordered systems [19,20] or when the screening radius is larger than the correlation length, i.e., the Cooper pair radius. This defines the difference between superconducting bulk metals, where the screening radius is of the order of the lattice constant such that the Coulomb interaction can be reasonably well described by a constant local Hubbard U, and slightly doped semiconductors, where the screening radius can be very large, which can become even more problematic in two dimensions (2D) as the screening properties of three-dimensional (3D) and 2D electron gases are essentially different [21–23].

For layered superconductors with reduced screening and hence naturally enhanced nonlocal Coulomb interactions it is thus *a priori* not clear whether the conventional local TMA pseudopotential is still a valid description or if a full treatment of the nonlocal Coulomb repulsion is required [24–26]. Nevertheless, the TMA pseudopotential has been regularly applied to study superconductors in 2D [27–37]. This together with numerous recent experiments on layered superconductors [38–42] motivates us to study here the effects of static long-range Coulomb interactions in conventional 2D superconductivity (dynamical Coulomb effects are discussed elsewhere see, e.g., Refs. [11], [43] or [12]). To this end we use the static Thomas-Fermi approximation of the Coulomb interaction, which coincides with the more accurate random phase approximation for $q < 2k_F$ for both parabolic [21] and Dirac [22,23] electronic spectra.

We find that a local approximation of the Coulomb interaction is actually still suitable to describe the relevant superconducting quantities even in the presence of long-range nonlocal static Coulomb interactions. We show, however, that the widely adopted TMA μ_C^* strongly overestimates the superconducting gap function at the Fermi level and thus the critical transition temperature. In the case of nonlocal Coulomb interactions, the screening effects resulting from virtual pair fluctuations at high energies *above* the Fermi level are strongly suppressed. This leads to a larger value of the screened TMA pseudopotential $\tilde{\mu}_C^*$, which in turn yields smaller

*m.roesner@science.ru.nl

superconducting gaps and reduced critical temperatures T_c. We derive a generalized expression for the evaluation of the new $\tilde{\mu}_C^*$, which takes into account the nonlocality of the static Coulomb interaction. Our expression elucidates quantitatively how the inverse screening length Λ and the chemical potential control the parameter $\tilde{\mu}_C^*$, and thus the critical temperature T_c. From this analysis it also emerges that the nonlocality of the Coulomb interaction is crucial for layered SCs with low carrier density (small Fermi energies) and small effective masses.

The paper is organized as follows. In Sec. II we introduce the extended 2D BCS model to account for the nonlocal Coulomb interaction. In Sec. III we present our main results obtained from numerical solutions of the extended gap equation. In Sec. IV we derive the Bethe-Salpeter equation describing the screening of the Coulomb interaction within the superconducting state due to virtual pair fluctuations from full nonlocal and dynamical Eliashberg equations and derive the generalized expression for $\tilde{\mu}_C^*$ which we compare to the numerical data. Section V summarizes our findings and highlights in which regime they are most important.

II. MODEL DEFINITIONS AND PROPERTIES

To study the effects of static nonlocal Coulomb interactions to the superconducting properties of a layered system, we solve the Hamiltonian

$$H = \sum_{\mathbf{k},\sigma} \xi_{\mathbf{k}} c^\dagger_{\mathbf{k}\sigma} c_{\mathbf{k}\sigma} + \sum_{\mathbf{k},\mathbf{k}'} [-g_{\mathbf{k}\mathbf{k}'} + V_{\mathbf{k}\mathbf{k}'}] c^\dagger_{\mathbf{k}\uparrow} c^\dagger_{-\mathbf{k}\downarrow} c_{-\mathbf{k}'\downarrow} c_{\mathbf{k}'\uparrow} \tag{1}$$

within mean-field BCS theory, where $c_{\mathbf{k}\sigma}$ ($c^\dagger_{\mathbf{k}\sigma}$) denotes the annihilation (creation) of a an electron with spin σ and momentum $\mathbf{k}$. $\xi_{\mathbf{k}} = \xi_k = \frac{\hbar^2 k^2}{2m^*} - \mu$ is a 2D electron gas dispersion with $k = |\mathbf{k}|$, μ the chemical potential, and m^* the effective mass. $g_{\mathbf{k}\mathbf{k}'}$ and $V_{\mathbf{k}\mathbf{k}'}$ describe the effective attractive interaction mediated by phonons and the static Coulomb repulsion between electrons, respectively. For the phonon mediated attraction we use the BCS model [4,44]

$$g_{\mathbf{k}\mathbf{k}'} = \begin{cases} g & \text{for } |\xi_{\mathbf{k}}| < \omega_D \text{ and } |\xi_{\mathbf{k}'}| < \omega_D, \\ 0 & \text{elsewhere} \end{cases} \tag{2}$$

which allows for electron paring within the Debye energy ω_D around the Fermi level. To understand the effects of nonlocal Coulomb repulsion we employ the static Thomas-Fermi (TF) approximation for the Coulomb interaction kernel $V_{\mathbf{k}\mathbf{k}'}$,

$$V_{\mathbf{k}\mathbf{k}'} = \frac{2\pi e^2}{\Omega} \frac{1}{\varepsilon |\mathbf{k} - \mathbf{k}'| + \Lambda}, \tag{3}$$

where Ω denotes the normalization area, e the electron charge, and ε a homogeneous local screening. We allow the TF wave vector $\Lambda_{\mathrm{TF}} = 4\pi e^2 \rho_0 / \Omega$ to be a free parameter Λ as it serves as a measure for the nonlocality. ρ_0 denotes the normal density of states at the Fermi level.

In order to understand the effects of static nonlocal Coulomb interaction on the gap function, this nonlocal BCS description represents a most convenient framework. To benchmark the accompanying BCS approximations, we further show numerically in Appendix C that our findings also hold for the general dynamical and nonlocal Eliashberg formalism.

For the BCS description we obtain after mean-field decoupling the gap equation

$$\Delta_{\mathbf{k}} = -\sum_{\mathbf{k}'} [-g_{\mathbf{k}\mathbf{k}'} + V_{\mathbf{k}\mathbf{k}'}] \frac{\tanh(\beta E_{\mathbf{k}'}/2)}{2E_{\mathbf{k}'}} \Delta_{\mathbf{k}'}, \tag{4}$$

where $E_{\mathbf{k}} = \sqrt{\xi_{\mathbf{k}}^2 + \Delta_{\mathbf{k}}^2}$ is the Bogoliubov dispersion relation and β the inverse temperature. In the presence of the nonlocal Coulomb interaction there are no analytical solutions known and we need to solve the gap function numerically. The common approximation to gain anyway analytical insights into the problem is by projecting the Coulomb kernel onto the Fermi surface via a double average of the form [7,8]

$$\mu_C = \langle\langle V_{\mathbf{k}\mathbf{k}'} \rangle\rangle_{\mathrm{FS}} = \frac{1}{\rho_0} \sum_{\mathbf{k},\mathbf{k}'} V_{\mathbf{k}\mathbf{k}'} \delta(\xi_{\mathbf{k}}) \delta(\xi_{\mathbf{k}'}) =: \rho_0 U, \tag{5}$$

where U describes an effective local interaction. We denote the gap function obtained with this local approximation by Δ_k^L, which can be analytically derived yielding [8,45]

$$\Delta_k^L = \begin{cases} \Delta_1^L & \text{for } |\xi_k| < \omega_D, \\ \Delta_2^L & \text{elsewhere} \end{cases} \tag{6}$$

with

$$\Delta_1^L = \frac{\omega_D}{\sinh\left(\frac{1}{\lambda - \mu_C^*}\right)} \quad \text{and} \quad \Delta_2^L = -\frac{\mu_C^*}{\lambda - \mu_C^*} \Delta_1^L. \tag{7}$$

Here $\lambda = \rho_0 g$ is the effective electron-phonon coupling strength and μ_C^* is the retarded Tolmachev-Morel-Anderson (TMA) pseudopotential defined by

$$\mu_C^* = \frac{\mu_C}{1 + \mu_C \log \frac{D}{\omega_D}}, \tag{8}$$

where D is the electron cutoff energy, which is typically of the order of the electron bandwidth [8,45]. The retarded pseudopotential μ_C^* is always smaller than the bare μ_C due to screening effects from virtual pair fluctuations at energies between ω_D and D. Thus, even for $\lambda - \mu_C < 0$ we can have $\lambda - \mu_C^* > 0$, i.e., a superconducting solution can exist. This underlines the importance of screening of the Coulomb repulsion by the high-energy degrees of freedom in this problem.

In the following we explore the validity of the local approximation of the Coulomb repulsion in the presence of a nonlocal Coulomb kernel and clarify the role of the nonlocality to the superconducting gap function, critical temperature T_c, and spectral function.

III. GAP FUNCTION STRUCTURE WITH LOCAL AND NONLOCAL COULOMB KERNELS

In Fig. 1 we show the gap function $\Delta_{\mathbf{k}} = \Delta_k$, as obtained from numerically solving Eq. (4) in polar coordinates (see Appendix A) with the full nonlocal Coulomb kernel $V_{\mathbf{k}\mathbf{k}'}$ and using $\hbar^2/m^* = 1$ Å^2 eV, $\mu = 0.5$ eV, $\lambda = 0.5$, $\omega_D = 75$ meV, $\Lambda = 1.5$ Å^{-1}, and $\varepsilon = 10$. The cutoff in k space is set to the Debye wave vector $k_D = \sqrt{4\pi}/a$ with $a = 3$ Å. For comparison we also show the analytical results for the

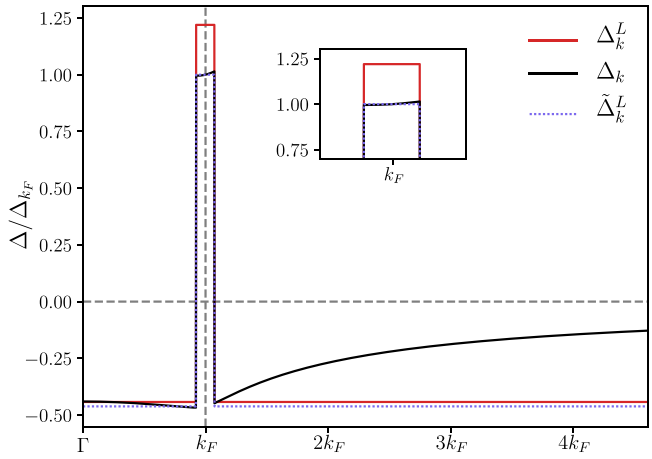

FIG. 1. Gap functions Δ_k and Δ_k^L obtained by solving the gap equation at $T = 0$ using the full nonlocal Coulomb kernel and a local one utilizing the conventional TMA pseudopotential μ_C^*, respectively. $\tilde{\Delta}_k^L$ represents the gap function with a local Coulomb kernel fitted to reproduce the Δ_k at k_F.

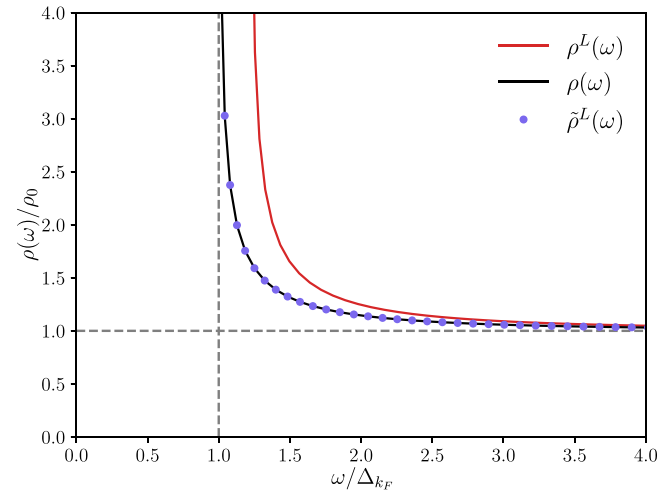

FIG. 3. Comparison of SC spectral functions $\rho(\omega)$, $\rho^L(\omega)$, and $\tilde{\rho}^L(\omega)$ resulting from Δ_k, Δ_k^L, and $\tilde{\Delta}_k^L$, respectively.

local approximation Δ_k^L from Eq. (6) using the Fermi-surface-averaged local Coulomb interaction from Eq. (5) yielding $\mu_C^* \approx 0.135$ via Eq. (8). From this comparison we find two important differences: (1) Similar to Δ_k^L, Δ_k also exhibits a separation into positive (low-energy) and negative (high-energy) components, but the nonlocality of the Coulomb repulsion induces a significant structure in the negative part (especially towards large k away from k_F) as well as a bending in the positive parts around k_F. (2) The conventional local approximation significantly overestimates the gap functions at the Fermi level, i.e., $\Delta_{k_F}^L > \Delta_{k_F}$, and also underestimates the negative parts.

In Fig. 2 we show both gap functions evaluated at the Fermi level $\Delta_{k_F}^L(T)$ and $\Delta_{k_F}(T)$ as functions of the temperature T. The data show that the conventional local approximation also significantly overestimates the critical temperature T_c of

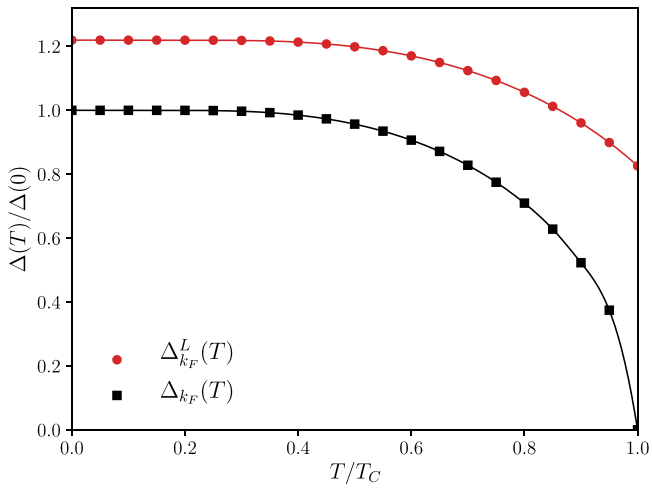

FIG. 2. Gap functions at k_F as function of temperature T. The temperature axis is normalized to the critical temperature T_c as predicted with BCS relation using $\Delta_{k_F}(0)$.

the nonlocal problem in perfect agreement with the full nonlocal and dynamical Eliashberg-type treatment discussed in Appendix C. Furthermore and even more important, we find that in the full nonlocal case T_c is related to zero-temperature value of the gap at the Fermi level $\Delta_{k_F}(0)$ by the BCS ratio $T_c = \frac{2\Delta_{k_F}(0)}{3.35}$.

This observation motivates us to *fit* the gap function Δ_k of the nonlocal interaction model with a gap function $\tilde{\Delta}^L$ of the form of Eq. (6), i.e., using a local Coulomb interaction. This gap $\tilde{\Delta}^L$ is constructed by adjusting μ_C^* in Eq. (7) such that $\tilde{\Delta}_{k_F}^L = \Delta_{k_F}$ holds. This yields a significantly *enhanced* $\tilde{\mu}_C^* \approx 0.157$ as compared to $\mu_C^* \approx 0.135$ calculated from Eq. (8). The resulting effective local model gap function at $T = 0$ is shown in Fig. 1, which yields by definition the same T_c as the full model. To further investigate the quality of this effective local model, which disregards all curvature of Δ_k, we calculate the interacting spectral functions $\rho(\omega) = \int dk\, \delta(\omega - E_k)$ for all three gap functions (Δ_k, Δ_k^L, and $\tilde{\Delta}_k^L$) and show them in Fig. 3.

We find that the full spectral function $\rho(\omega)$ can be accurately approximated by the spectral function $\tilde{\rho}^L(\omega)$ obtained from the fitted local interaction model. Thus, the curvature of Δ_k does not have a major impact to the spectral function, which has a twofold reason: the bending in Δ_k within the low-energy region around k_F is rather small and does not affect strongly the coherence peaks. Second, as soon as $|\xi| > \omega_D$ the detailed structure of $\Delta_k \ll \omega_D$ does not affect the Bogoliubov dispersion $E = \sqrt{\xi^2 + \Delta^2}$ anymore. The negative component of Δ_k thus leaves no significant trace in the spectral function.

This analysis shows that within the BCS framework the value of the gap function at k_F is sufficient for the evaluation of the relevant SC quantities in layered materials. However, the data also show that in this generic model the commonly adopted TMA approach always overestimates the value of the gap function at the Fermi level and therefore overestimates the critical temperature T_c as it underestimates μ_C^*. The nonlocal Coulomb interactions thus reduce the gap function at the Fermi level.

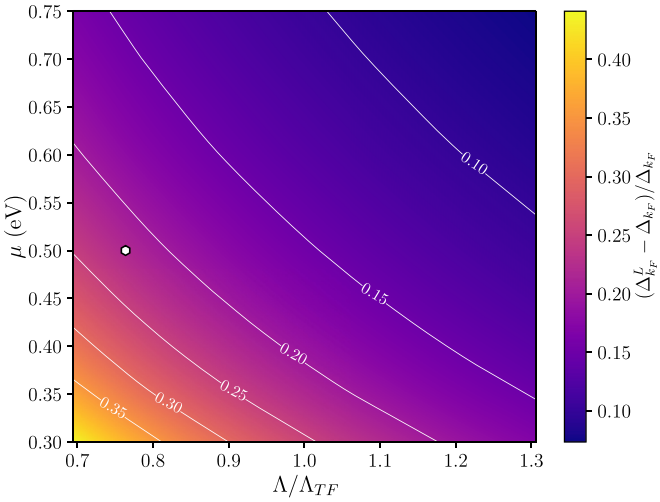

FIG. 4. Relative difference between $\Delta^L_{k_F}$ and Δ_{k_F} as a function of inverse screening length $\Lambda/\Lambda_{\mathrm{TF}}$, and chemical potential μ. Here the white marker denotes the parameters (Λ, μ) as used for the data shown in Figs. 1–3.

This is indeed generic as depicted in Fig. 4 where we show the relative difference between the full Δ_{k_F} and the conventional local TMA approximation $\Delta^L_{k_F}$. This deviation is controlled by the inverse screening length Λ as well as by the chemical potential μ. As Λ decreases, the nonlocality in the Coulomb interaction becomes stronger and thus we find larger differences between Δ_{k_F} and $\Delta^L_{k_F}$. Interestingly, the deviation is also found to increase for smaller chemical potentials. These trends to Δ_{k_F} and $\Delta^L_{k_F}$ and thus T_c and T^L_c are again in perfect agreement with the full nonlocal and dynamical Eliashberg-type treatment discussed in Appendix C. In the next section, the analysis of the Bethe-Salpeter equation will reveal the physical reasons determining this behavior and provides an accurate quantitative description.

IV. BETHE-SALPETER EQUATION AND REVISED TOLMACHEV-MOREL-ANDERSON POTENTIAL

From the previous analysis we understand that a local Coulomb interaction model can accurately reproduce the gap function of the full nonlocal Coulomb model at k_F, which controls most relevant SC quantities. The possibility to employ a local Coulomb kernel is a significant simplification of the problem, as the gap function at the Fermi level admits in this case a simple analytical solution (6). We therefore aim to understand the nature of the parameter $\tilde{\mu}^*_C$, which is responsible for the deviation between Δ_{k_F} and $\tilde{\Delta}^L_{k_F}$.

The discrepancy between μ^*_C and the correct value $\tilde{\mu}^*_C$ is to be attributed to the role of nonlocality of the Coulomb interaction in the retardation effects. In order to understand this, we study the Eliashberg equations in the presence of dynamic phonon-mediated interaction and *static* but *nonlocal* Coulomb repulsion. Hence, in this model the Coulomb interaction is approximated to be frequency independent. We closely follow Vonsovsky *et al.* [4] (see also Pellegrini *et al.* [24]) and start from the Eliashberg equation for the anomalous self-energy $\phi_{\mathbf{k}}(\omega) = \phi^{\mathrm{ph}}_{\mathbf{k}}(\omega) + \phi^{\mathrm{C}}_{\mathbf{k}}$, which reads as in spectral representation

$$\phi^{\mathrm{ph}}_{\mathbf{k}}(\omega) = -\sum_{\mathbf{k}'} \int dz' \int dz\, |g_{\mathbf{k}\mathbf{k}'}|^2\, b_{\mathbf{k}\mathbf{k}'}(z) \frac{\tanh\frac{\beta z'}{2} + \coth\frac{\beta z}{2}}{\omega + i\eta - z - z'} \mathrm{Im} \frac{\phi_{\mathbf{k}'}(z')}{[Z_{\mathbf{k}'}(z')z']^2 - \xi^2_{\mathbf{k}'} - \phi^2_{\mathbf{k}'}(z')}, \tag{9}$$

$$\phi^{\mathrm{C}}_{\mathbf{k}} = -\sum_{\mathbf{k}'} \int dz'\, V_{\mathbf{k}\mathbf{k}'} \tanh\frac{\beta z'}{2} \mathrm{Im} \frac{\phi_{\mathbf{k}'}(z')}{[Z_{\mathbf{k}'}(z')z']^2 - \xi^2_{\mathbf{k}'} - \phi^2_{\mathbf{k}'}(z')}, \tag{10}$$

where $g_{\mathbf{k}\mathbf{k}'}$ is the electron-phonon coupling, $b_{\mathbf{k}\mathbf{k}'}(z)$ the phonon spectral function, $V_{\mathbf{k}\mathbf{k}'}$ the static nonlocal Coulomb interaction, and $Z_{\mathbf{k}}(z)$ the mass renormalization function. For our discussion we focus on Eq. (10) defining the Coulomb component ϕ^{C}. Since $Z_{\mathbf{k}}(z)$ is resulting from the phonon properties only it becomes $Z_{\mathbf{k}}(z) = 1$ above a cutoff energy ω_c where the phonon component ϕ^{ph} furthermore vanishes. This allows us to split the frequency integration domain into a low-energy domain Γ_1 with $|z| < \omega_c$ and a high-energy domain Γ_2 with $|z| > \omega_c$ yielding

$$\phi^{\mathrm{C}}_{\mathbf{k}} = -\sum_{\mathbf{k}'} \left[\int_{\Gamma_1} dz'\, V_{\mathbf{k}\mathbf{k}'} \tanh\frac{\beta z'}{2} \mathrm{Im} \frac{\phi_{\mathbf{k}'}(z')}{[Z_{\mathbf{k}'}(z')z']^2 - \xi^2_{\mathbf{k}'} - \phi^2_{\mathbf{k}'}(z')} + \int_{\Gamma_2} dz' V_{\mathbf{k}\mathbf{k}'} \tanh\frac{\beta z'}{2} \mathrm{Im} \frac{\phi^{\mathrm{C}}_{\mathbf{k}'}}{[z']^2 - \xi^2_{\mathbf{k}'} - \left[\phi^{\mathrm{C}}_{\mathbf{k}'}\right]^2} \right].$$

For every $z' \in \Gamma_2$ we have $\tanh\frac{\beta z'}{2} \to 1$ since $\omega_c \gg T_c$ and $E^2_{\mathbf{k}} = \xi^2_{\mathbf{k}} + [\phi^C_{\mathbf{k}}]^2$. This allows us to perform the integral in Γ_2 exactly yielding

$$\phi^{\mathrm{C}}_{\mathbf{k}} = -\sum_{\mathbf{k}'} \left[\int_{\Gamma_1} dz'\, V_{\mathbf{k}\mathbf{k}'} \tanh\frac{\beta z'}{2} \mathrm{Im} \frac{\phi_{\mathbf{k}'}(z')}{[Z_{\mathbf{k}'}(z')z']^2 - \xi^2_{\mathbf{k}'} - \phi^2_{\mathbf{k}'}(z')} + V_{\mathbf{k}\mathbf{k}'} \frac{\phi^{\mathrm{C}}_{\mathbf{k}'}}{2|E_{\mathbf{k}'}|} \theta(|E_{\mathbf{k}'}| - \omega_c) \right]. \tag{11}$$

Conventional TMA approach:

$$V_{\mathbf{kk}'} \rightarrow \boxed{\text{FS projection}} \rightarrow \mu_C \rightarrow \boxed{\text{BSE}} \rightarrow \mu_C^*$$

Revised approach:

$$V_{\mathbf{kk}'} \rightarrow \boxed{\text{BSE}} \rightarrow W_{\mathbf{kk}'} \rightarrow \boxed{\text{FS projection}} \rightarrow \tilde{\mu}_C^*$$

FIG. 5. Schematic representation of the conventional TMA approach in contrast to our revised approach to evaluate the retarded potential.

To solve this equation, we utilize an ansatz of the following form:

$$\phi_{\mathbf{k}}^{\mathrm{C}} = \int_{\Gamma_1} dz' \sum_{\mathbf{k}'} W_{\mathbf{kk}'} \tanh\frac{\beta z'}{2} \operatorname{Im}\frac{\phi_{\mathbf{k}'}(z')}{[Z_{\mathbf{k}'}(z')z']^2 - \xi_{\mathbf{k}'}^2 - \phi_{\mathbf{k}'}^2(z')},$$

which we plug into Eq. (11). Relabeling the momentum index we find a self-consistent Bethe-Salpeter equation defining the screeened Coulomb potential $W_{\mathbf{kk}'}$,

$$W_{\mathbf{kk}'} = V_{\mathbf{kk}'} - \sum_{\mathbf{q}\in\bar{\chi}} V_{\mathbf{kq}} \frac{1}{2|\xi_{\mathbf{q}}|} W_{\mathbf{qk}'}, \tag{12}$$

where $E_{\mathbf{k}} \sim \xi_{\mathbf{k}}$ for energies larger than $\omega_c \sim \omega_D$, and the domain $\bar{\chi}$ denotes $\mathbf{q}$ such that $|\xi_{\mathbf{q}}| > \omega_D$. This BSE describes the screening of the Coulomb interaction due to fluctuations of virtual pairs, and can be diagrammatically depicted as

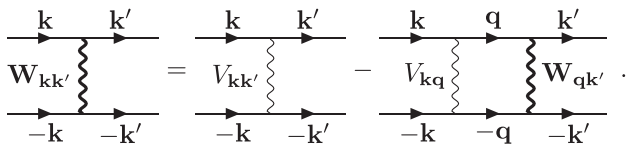

For a local potential $V_{\mathbf{kk}'} = U$ one obtains the conventional retarded TMA potential μ_C^* in the form of Eq. (8).

The total $\phi_{\mathbf{k}}(i\omega_n)$ is thus *solely* determined by an integral over the low-frequency domain Γ_1, which shows that the details of the specific dynamic phonon-mediated interaction are irrelevant in determining the screening of the bare static nonlocal Coulomb kernel.

From our previous analysis we understand that a single parameter $\tilde{\mu}_C^*$ is capable to encode the relevant retardation effects affecting the energy gap *at the Fermi level*. To correctly account for this it is therefore necessary to evaluate the retarded (nonlocal) potential $W_{\mathbf{kk}'}$ first, and only subsequently project it onto the Fermi surface. This procedure is depicted schematically in Fig. 5. By commuting the conventional order of operations, which is normally employed to estimate μ_C^*, we ensure that the nonlocal screening effects due to high-energy virtual pair fluctuations are evaluated *before* the potential is projected onto the Fermi surface.

In 2D and for isotropic dispersion relations $\xi_{\mathbf{q}} = \xi_q$ and isotropic Coulomb kernels $V_{\mathbf{kk}'} = V_{kk'}$, we can perform this approach analytically to obtain an explicit expression for $\tilde{\mu}_C^*$. To this end, we introduce the reduced angle-integrated BSE (at $T = 0$), with $z_{kk'} = \frac{f_{kk'}}{U}$ and $z_{kk'}^* = \frac{f_{kk'}^*}{U}$, and project onto the Fermi surface:

$$z_{k_Fk_F}^* = z_{k_Fk_F} - U\int_{\bar{\chi}} dq\, z_{k_Fq} \frac{1}{2|\xi_q|} z_{qk_F}^*, \tag{13}$$

where $f_{kk'}$ and $f_{kk'}^*$ are the angle-integrated versions of $V_{\mathbf{kk}'}$ and $W_{\mathbf{kk}'}$, respectively (see Appendix A). To solve this self-consistent equation we choose an ansatz of the form $z_{k_Fq}^* = \alpha z_{k_Fq}$ and obtain

$$\alpha = \frac{1}{1+\mu_C\gamma}, \tag{14}$$

with

$$\gamma = \frac{1}{\rho_0}\int_{\bar{\chi}} dq \frac{z_{k_Fq}^2}{2|\xi_q|}. \tag{15}$$

This finally yields the revised retarded potential

$$\tilde{\mu}_C^* = \frac{\mu_C}{1+\mu_C\gamma}. \tag{16}$$

This result is a generalization of the TMA potential μ_C^*, which now takes into account the effect of nonlocal screening in the BSE. In the local limit $z_{k_Fq} = 1$ (large Λ and large μ) γ immediately yields

$$\gamma = \int_{\omega_D}^{D} d\xi \frac{1}{|\xi|} = \log\left(\frac{D}{\omega_D}\right), \tag{17}$$

such that $\tilde{\mu}_C^*$ correctly reduces to μ_C^* as in Eq. (8). In Fig. 6 we analyze the quality of the revised $\tilde{\mu}_C^*$ by comparing it with the optimal μ_C^*, which is obtained by inverting the relation from Eq. (6) using the numerically obtained Δ_{k_F}. Additionally, we show the comparison with the conventional TMA pseudopotential μ_C^*. The qualitative and quantitative agreement between the numerically obtained optimal value and our revised approximation is very good for all Λ as well as for different μ, even for small values of Λ, where the nonlocality of the Coulomb interaction is strong.

In order to understand why $\tilde{\mu}_C^* > \mu_C^*$ we need to analyze γ from Eq. (15) and therefore the function $z_{k_Fk}^2$. To this end we show in Fig. 7 $z_{k_Fk}^2$ for different values of Λ and chemical potential μ. We notice that this function is approximately constant for the states below the Fermi level and rapidly decays for the states *above* it. Thus, in the presence of nonlocal interactions, pair fluctuations involving occupied sates below the Fermi level contribute to the screening (retardation) as in the case of a local potential, whereas the effects of screening from pair fluctuations involving unoccupied states above the Fermi level are strongly suppressed, as dictated by the decay of $z_{k_Fk}^2$ for large momenta k. It is furthermore important to note that γ not only depends on the inverse screening length Λ, but also strongly depends on the chemical potential μ through $z_{k_Fk}^2$. This is different to the conventional case, where the chemical potential does not control directly the screening effects. This eventually explains the trends we observed in Fig. 4, where the discrepancy between $\tilde{\mu}_C^*$ and μ_C^* increases for smaller chemical potential.

V. DISCUSSION

Our results show that nonlocal Coulomb interactions can have a strong effect to superconducting properties by, e.g.,

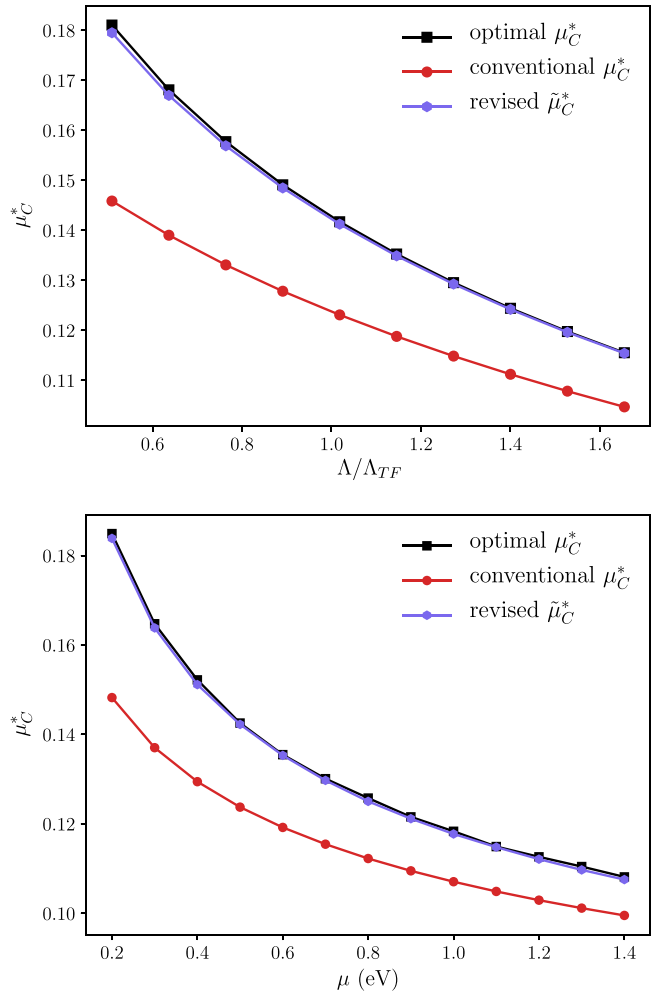

FIG. 6. Comparison of the conventional TMA μ_C^* and the revised $\tilde{\mu}_C^*$ with numerically obtained optimal μ_C^* as a function of $\Lambda/\Lambda_{\mathrm{TF}}$ (upper panel) and μ (lower panel).

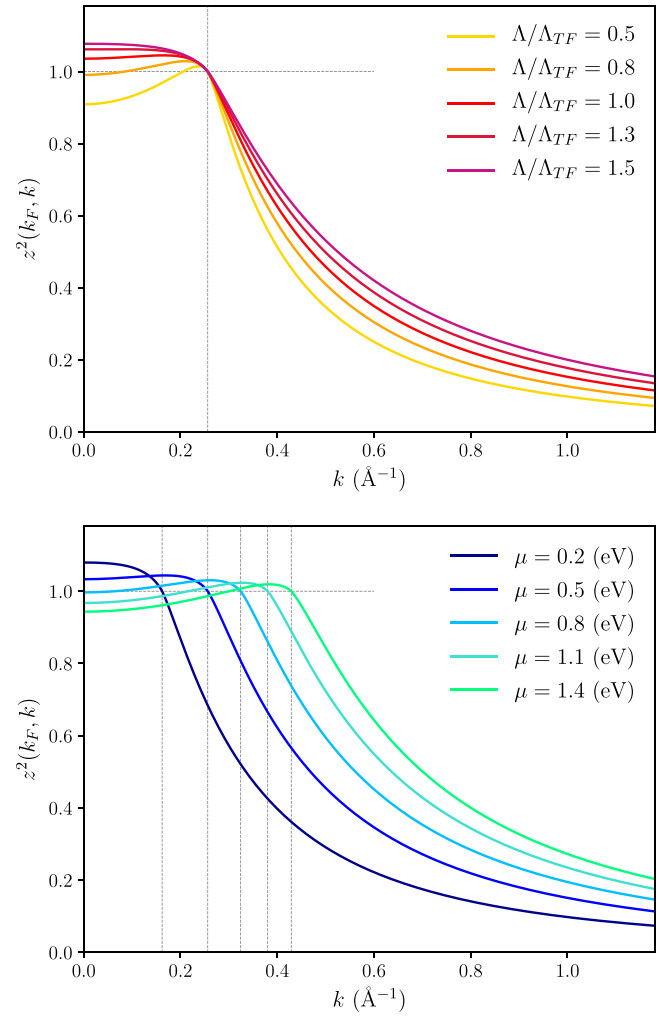

FIG. 7. The function $z^2(k_F, k)$ for $\mu = 0.5$ eV and different Λ (top panel) and for $\Lambda/\Lambda_{\mathrm{TF}} = 1.0$ and different μ (bottom panel). The vertical dashed lines denote k_F.

suppressing T_c. In this context the *ab initio* study on doped layered nitrides by Akashi *et al.* [25] is interesting to note. In this work, the authors derived the superconducting transition temperatures in two ways: (a) via the McMillan-Allen-Dynes (MAD) formula for which they calculate all necessary parameters from *ab initio* including the *local* retarded TMA Coulomb pseudopotential μ_C^* and (b) directly via density functional theory for superconductors (SC-DFT) using the full nonlocal Coulomb interaction. Upon neglecting the Coulomb repulsion Akashi *et al.* find these two approaches to be in good agreement. However, upon taking the Coulomb repulsion into account they consistently find $T_c^{\text{SC-DFT}} < T_c^{\text{MAD}}$. The conventional *local* retarded Coulomb pseudopotential μ_C^* thus tends to overestimate the critical temperature or, vice versa, the nonlocal Coulomb interaction seems to suppress superconductivity. Similar trends have also been found from solutions to Eliashberg equations considering the full momentum dependence of the static Coulomb interaction within layered CaC_6 and LiZrNCl [24]. These observations are fully inline with our findings here. We expect that using our revised $\tilde{\mu}_C^*$ within the MAD formula will result in $T_c^{\text{SC-DFT}} \approx T_c^{\text{MAD}}$ and can reproduce the results from Pellegrini *et al.* [24].

In this context experimental data on superconducting transition metal dichalcogenides (TMDCs) is additionally interesting to note. For MoS_2 [46,47] and $NbSe_2$ [48–50] there is a consistent drop in T_c in their monolayer limits compared to their multilayer compounds. While hybridization and substrate effects might play a role to describe this behavior [28,51], it might (at least partially) also result from the enhanced long-range Coulomb interaction in the monolayer limit, which is suppressed in the multilayer compounds.

VI. CONCLUSION AND OUTLOOK

We analyzed the behavior of conventional two-dimensional superconductors subject to static nonlocal Coulomb interactions within both an extended nonlocal BCS model for a numerical benchmark and a more general nonlocal and dynamical Eliashberg-type framework. We found that the nonlocal Coulomb interaction leads to modifications to the superconducting gap function in momentum space, most importantly, in form of a reduced negative amplitude at large momenta away from the Fermi surface. Upon numerically

and analytically analyzing the Bethe-Salpeter equation (BSE) describing the screening of the bare Coulomb repulsion by pair fluctuations, we understood that high-energy screening processes are suppressed in the case of nonlocal Coulomb interactions, which effectively enhances the Coulomb repulsion and thus suppresses superconductivity.

We demonstrate that the widely applied Fermi-surface averaged Tolmachev-Morel-Anderson *local* Coulomb pseudopotential μ_C^* overestimates the BSE screening, yielding to too small Coulomb repulsion and thus too large superconducting gaps and transition temperatures as soon as nonlocal Coulomb interactions are present. This finding is in line with numerical data by Akashi *et al.* showing that the TMA μ_C^* overestimates T_c in layered nitrides [25].

Finally, we reanalyzed the BSE in the presence of nonlocal Coulomb repulsion and were able to derive a revised Tolmachev-Morel-Anderson *local* Coulomb pseudopotential $\tilde{\mu}_C^*$, which takes into account the reduced screening at high energies. This $\tilde{\mu}_C^*$ allows to quantitatively approximate the gap function from the full nonlocal Coulomb kernel at the Fermi level. The existence of such a refined *local* pseudopotential is an important finding on its own, as it allows it to be an effective fitting parameter to reproduce experimental data even without microscopic knowledge of the Coulomb interactions. Furthermore, in case one has access to the microscopic Coulomb interaction $V_{kk'}$, our refined $\tilde{\mu}_C^*$ is relatively easy to evaluate. Nevertheless, we need to note that the onset of a finite gap function must not necessarily coincide with the onset of superconductivity in layered systems. The difference between T_c and the relevant Berezinsky-Kosterlitz–Thouless transition temperature for mildly anisotropic layered superconductors can be on the order of a few percent [52,53].

As in layered materials environmental screening is in general reduced, we expect our findings to be most important for conventional superconductivity in thin-film metals in two ways: (1) superconducting properties including transition temperatures are likely reduced in the thin-film limit due to strong internal nonlocal Coulomb interactions and weak external screening; (2) environmental or substrate screening to thin-film superconductors could be beneficial as it generally reduces the bare Coulomb repulsion in the thin-film superconductor and reduces its long-range character. Thus, environmental screening will effectively decrease the nonlocality of the Coulomb repulsion, which, according to our findings presented here, should enhance T_c.

Furthermore, our findings show that nonlocal Coulomb interaction effects are important at reduced Fermi levels. We thus expect the nonlocal Coulomb interaction to reduce superconducting properties mostly in slightly doped layered semiconducting systems with small effective masses. This might be one of the reasons why the critical temperatures in monolayers of doped MoS_2 and WS_2 are reduced compared to their multilayer counterparts.

ACKNOWLEDGMENTS

We acknowledge fruitful discussions with Y. in't Veld, T. Westerhout, A. J. Millis, B. V. Svistunov, N. V. Prokof'ev, and A. Chubukov. We especially thank Y. in't Veld for supporting the numerical Eliashberg calculations. M.R. and M.I.K. acknowledge support from the Dutch Research Council (NWO) via the "TOPCORE" consortium as well as partial support by the European Commission's Horizon 2020 RISE program Hydrotronics (Grant No. 873028) and the research program "Materials for the Quantum Age" (QuMat). This program (registration no. 024.005.006) is part of the Gravitation program financed by the Dutch Ministry of Education, Culture and Science (OCW). The work of M.I.K. was further supported by the European Research Council (ERC) under the European Union's Horizon 2020 research and innovation programme, Grant Agreement No. 854843-FASTCORR.

APPENDIX A: POLAR COORDINATES REPRESENTATION

The Coulomb interaction in polar coordinates reads as

$$V(k,k',\theta,\theta') = \frac{2\pi e^2}{\Omega}\frac{1}{\epsilon\sqrt{k^2+k'^2-2kk'\cos(\theta-\theta')}+\Lambda}, \tag{A1}$$

which allows us to define the angle-integrated interaction as

$$f_{kk'} := \int_0^{2\pi}\frac{d\theta}{2\pi}\int_0^{2\pi}\frac{d\theta'}{2\pi}V(k,k',\theta,\theta'). \tag{A2}$$

With $\phi = \theta + \theta'$ and $\phi = \theta - \theta'$ we can evaluate

$$f_{kk'} = 2\int_0^{2\pi}\frac{d\phi'}{2\pi}\int_0^{\phi'}\frac{d\phi}{2\pi}\frac{2\pi e^2/\Omega}{\epsilon\sqrt{k^2+k'^2-2kk'\cos\phi}+\Lambda} \tag{A3}$$

$$= \int_0^{2\pi}\frac{d\phi}{2\pi}\frac{2\pi e^2/\Omega}{\epsilon\sqrt{k^2+k'^2-2kk'\cos\phi}+\Lambda}. \tag{A4}$$

The gap equation at $T = 0$ then takes the form

$$\Delta_k = \frac{\Omega}{2\pi}\int dk'k'[g_{kk'} - f_{kk'}]\frac{\Delta_{k'}}{2E_{k'}}. \tag{A5}$$

In polar representation the conventional Coulomb potential from Eq. (5) is given by

$$\mu_C = \rho_0 f_{k_F k_F} =: \rho_0 U. \tag{A6}$$

We note that the isotropic 2D system is a particular case, as only here we can readily derive the angle-integrated BSE in form Eq. (13).

APPENDIX B: ANALYTICAL SOLUTION OF THE GAP EQUATION

In the case of a local Coulomb interaction the gap equation from Eq. (6) leads to the system of equations

$$\Delta_1 = (g-U)\int_\chi dk\frac{\Delta_1}{2\sqrt{(\xi_k^2+\Delta_1^2)}} - U\int_{\bar{\chi}} dk\frac{\Delta_2}{2|\xi_k|},$$

$$\Delta_2 = -U\int_\chi dk\frac{\Delta_1}{2\sqrt{(\xi_k^2+\Delta_1^2)}} - U\int_{\bar{\chi}} dk\frac{\Delta_2}{2|\xi_k|},$$

which yield after integration

$$\Delta_1 = (g-U)\Delta_1\rho_0 \text{arsinh}\left(\frac{\omega_D}{\Delta_1}\right) - U\Delta_2\rho_0 \log\left(\frac{D}{\omega_D}\right),$$
$$\Delta_2 = -U\Delta_1\rho_0 \text{arsinh}\left(\frac{\omega_D}{\Delta_1}\right) - U\Delta_2\rho_0 \log\left(\frac{D}{\omega_D}\right).$$

This system of equations is solved by the expression from Eq. (7).

In the case of nonlocal Coulomb interactions, we know the gap function exhibits a structure in momentum space. However, the domain χ where $|\xi_k| < \omega_D$ is typically much smaller than $\bar{\chi}$. This allows us to neglect any k dependence of the gap function within the region χ, and approximate it with $\tilde{\Delta}_{k_F} =: \tilde{\Delta}_1$. By denoting the negative part of the energy gap with $\Delta_2(k)$ the angle-integrated gap equation reads as

$$\tilde{\Delta}_1 = g\int_\chi dk' \frac{\tilde{\Delta}_1}{2\sqrt{(\xi_{k'}^2+\tilde{\Delta}_1^2)}} - \int_\chi dk' f_{k_F k'} \frac{\tilde{\Delta}_1}{2\sqrt{(\xi_{k'}^2+\tilde{\Delta}_1^2)}} - \int_{\bar{\chi}} dk' f_{k_F k'} \frac{\Delta_2(k')}{2|\xi_{k'}|}, \tag{B1}$$

$$\Delta_2(k) = -\int_\chi dk' f_{kk'} \frac{\tilde{\Delta}_1}{2\sqrt{(\xi_{k'}^2+\tilde{\Delta}_1^2)}} - \int_{\bar{\chi}} dk' f_{kk'} \frac{\Delta_2(k')}{2|\xi_{k'}|}. \tag{B2}$$

To proceed we define the dimensionless gap $\delta(k) := \Delta_2(k)/\tilde{\Delta}_1$ and search for a solution with the ansatz

$$\delta(k) = -\alpha f_{k_F k},$$

where α is a scalar. By approximating $f_{kk'}$ with $f_{kk'_F}$ for $k' \in \chi$ in the first term of the right-hand side and employing the isotropy $f_{k_F k} = f_{kk_F}$, we finally arrive at the expression

$$\alpha = \frac{\rho_0 \text{arsinh}\left(\frac{\omega_D}{\tilde{\Delta}_1}\right)}{1 + \frac{1}{f_{k_F k}}\int_{\bar{\chi}} f_{kk'} f_{k_F k'} \frac{1}{2|\xi|}}. \tag{B3}$$

α is here still a function of the external variable k, thus a scalar α cannot provide a full solution for all k. However, we find (1) for large values of $k = \bar{k}$, the function $f_{\bar{k}k'}$ becomes approximately constant. This means that we can approximate $f_{\bar{k}k'}$ with $f_{\bar{k}k_F}$ and obtain an asymptotically correct approximation for $\Delta_2(k)$ in the nonlocal interaction model:

$$\delta(\bar{k}) = -\frac{\mu_C}{1+\mu_C\gamma_1} z_{k_F\bar{k}} \text{arsinh}\left(\frac{\omega_D}{\tilde{\Delta}_1}\right),$$

where $z_{k_F k} = \frac{f_{k_F k}}{U}$ and the coefficient γ_1 is defined

$$\gamma_1 = \frac{1}{\rho_0}\int_{\bar{\chi}} dk \frac{z(k_F,k)}{2|\xi_k|}.$$

(2) Most importantly, Eq. (B3) allows us to evaluate $\tilde{\Delta}_1$ by estimating the screening (retardation) effects of the high-energy pair fluctuations *acting at the Fermi level*. This is achieved by setting $k = k_F$ in Eq. (B3) such that we get

$$\alpha = \frac{1}{1+\mu_C\gamma}\rho_0 \text{arsinh}\left(\frac{\omega_D}{\tilde{\Delta}_1}\right)$$

with

$$\gamma = \frac{1}{\rho_0}\int_{\bar{\chi}} dk\, z^2(k_F,k)\frac{1}{2|\xi_k|}.$$

This yields with Eq. (B1)

$$1 = \left[\lambda - \frac{\mu_C}{1+\mu_C\gamma}\right]\text{arsinh}\left(\frac{\omega_D}{\tilde{\Delta}_1}\right),$$

which allows us to identify the revised TMA pseudopotential $\tilde{\mu}_C^*$ as

$$\tilde{\mu}_C^* = \frac{\mu_C}{1+\mu_C\gamma}.$$

This result is consistent with the one we obtained by analyzing the Bethe-Salpeter equation.

APPENDIX C: T_C FROM NUMERICAL SOLUTION OF ELIASHBERG EQUATION WITH NONLOCAL COULOMB INTERACTION

To further analyze the generality of our results we solve an Eliashberg-type gap equation for a one-band model with quadratic dispersion and obtain T_c in the presence of a static nonlocal Coulomb interaction $V_{kk'}$ and local electron-phonon coupling. The general linearized equation for the anomalous self-energy $\phi(k, i\omega_n)$ without mass-enhancement terms in Matsubara frequencies reads as

$$\phi_k(i\omega_m) = \frac{1}{\beta}\sum_n\sum_{k'}[D_{kk'}(i\omega_m - i\omega_n) - V_{kk'}]\frac{\phi_{k'}(i\omega_n)}{[i\omega_n]^2 - \xi_{k'}^2}, \tag{C1}$$

where $D_{kk'}(i\nu_n)$ denotes the phonon-mediated interaction. We use here a local Einstein phonon model of the form

$$D_{kk'}(i\nu_n) = D(i\nu_n) = g^2\frac{2\omega_0}{{i\nu_n}^2 - \omega_0^2}, \tag{C2}$$

with $\omega_0 = 0.3$ eV and a local electron-phonon interaction of $g^2 = 1.25\ \text{eV}^2$. We solve this linearized equation as an eigenvalue equation for ϕ. The critical temperature T_c is defined as the temperature at which the leading eigenvalue becomes unity. The calculations are performed for a quadratic band with $\hbar^2/m^* = 1\ \text{Å}^2\,\text{eV}$ on 320×320 k and q grids, using a Matsubara frequency cutoff of 10 eV, a k-space cutoff of $\pi/0.65\ \text{Å}^{-1}$ utilizing a 2D solver we recently implemented [43] within Triqs [54] and Tprf [55]. We proceed in analogy with our investigation of the static BCS model and compare T_c of the two different cases of nonlocal interaction $V_{kk'}$ at $\varepsilon = 30$ and local interaction $U = \mu_c/\rho_0$. To this end, we calculate μ_c for the nonlocal interactions $V_{kk'}$ using Eq (A6) yielding

$$\mu_C = \frac{\rho_0 e^2}{\Omega\epsilon k_F} I\left(\frac{\Lambda}{2k_F\epsilon}\right), \tag{C3}$$

with

$$I(x) = \int_0^\pi d\theta \frac{1}{\sin\theta + x} = \frac{2}{\sqrt{x^2-1}}\left[\frac{\pi}{2} - \arctan\left(\frac{1}{\sqrt{x^2-1}}\right)\right].$$

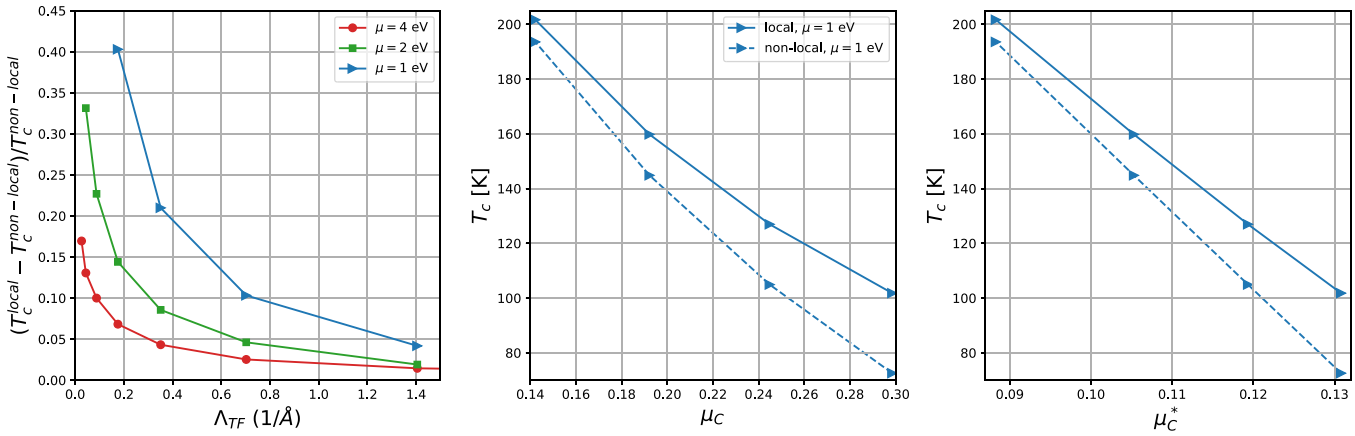

FIG. 8. Left panel: Normalized deviation of T_c^{nonlocal} from T_c^{local}, as a function of TF inverse wavelength Λ and chemical potential μ. The comparison is taken at fixed value of μ_C, obtained via FS projection. Center and right panels: Comparison of T_c in the local and nonlocal cases for $\mu = 1$ eV, as function of μ_C and of μ_C^* as expected from the conventional TMA formula.

The resulting comparison is shown in Fig. 8. The data show that the T_c obtained with the nonlocal interaction is always smaller than the one obtained with the local interaction. Moreover, the deviation from the conventional approach is enhanced for smaller chemical potential, as shown in the analysis of the $z(k_F, q)$ function in the main text. We note that the extent of the deviation is quantitatively in line with the results obtained from the BCS gap function at $T = 0$, as presented in Fig. 4. From the right panel of Fig. 8, we understand that an adequate $\tilde{\mu}_C^*$ value to approximate T_c in the nonlocal case with the help of an effective local model needs to be larger than the usual μ_C^*

These numerical results obtained in the framework of a general nonlocal and dynamical theory complement the analytical derivation in Sec. IV and show that the role of static nonlocality in the Coulomb repulsion is independent from the specific details of the phonon model for conventional phonon-mediated superconductors. This is in excellent agreement with our BCS-based derivation and discussion in the main text.

[1] G. M. Eliashberg, Zh. Eksper. Teor. Fiz. **38**, 966 (1960) [Sov. Phys.–JETP **11**, 696 (1960)].
[2] J. P. Carbotte, Rev. Mod. Phys. **62**, 1027 (1990).
[3] P. B. Allen and B. Mitrović, Solid State Phys. **37**, 1 (1983).
[4] S. V. Vonsovsky, Y. A. Izyumov, and E. Z. Kurmaev, *Superconductivity of Transition Metals: Their Alloys and Compounds* (Springer, Berlin, 2011).
[5] A. Secchi, M. Polini, and M. I. Katsnelson, Ann. Phys. **417**, 168100 (2020).
[6] A. O. Anokhin and M. I. Katsnelson, Int. J. Mod. Phys. B **10**, 2469 (1996).
[7] N. N. Bogoliubov, V. V. Tolmachev, and D. V. Shirkov, *A New Method in the Theory of Superconductivity* (Consultants Bureau, New York, 1959); V. V. Tolmachev, Dokl. Akad. Nauk SSSR **140**, 563 (1961).
[8] P. Morel and P. W. Anderson, Phys. Rev. **125**, 1263 (1962).
[9] J. Bauer, J. E. Han, and O. Gunnarsson, Phys. Rev. B **87**, 054507 (2013).
[10] R. Akashi, Phys. Rev. B **105**, 104510 (2022).
[11] T. Wang, X. Cai, K. Chen, B. V. Svistunov, and N. V. Prokof'ev, Phys. Rev. B **107**, L140507 (2023).
[12] A. Davydov, A. Sanna, C. Pellegrini, J. K. Dewhurst, S. Sharma, and E. K. U. Gross, Phys. Rev. B **102**, 214508 (2020).
[13] R. Akashi and R. Arita, Phys. Rev. Lett. **111**, 057006 (2013).
[14] A. Bill, H. Morawitz, and V. Z. Kresin, Phys. Rev. B **68**, 144519 (2003).
[15] C. F. Richardson and N. W. Ashcroft, Phys. Rev. B **55**, 15130 (1997).
[16] Y. Takada, Phys. Rev. B **47**, 5202 (1993).
[17] H. Rietschel and L. J. Sham, Phys. Rev. B **28**, 5100 (1983).
[18] Y. Takada, J. Phys. Soc. Jpn. **45**, 786 (1978).
[19] P. W. Anderson, K. A. Muttalib, and T. V. Ramakrishnan, Phys. Rev. B **28**, 117 (1983).
[20] L. N. Bulaevskii and M. V. Sadovskii, J. Low Temp. Phys. **59**, 89 (1985).
[21] T. Ando, A. B. Fowler, and F. Stern, Rev. Mod. Phys. **54**, 437 (1982).
[22] V. N. Kotov, B. Uchoa, V. M. Pereira, F. Guinea, and A. H. Castro Neto, Rev. Mod. Phys. **84**, 1067 (2012).
[23] M. I. Katsnelson, *The Physics of Graphene*, 2nd ed. (Cambridge University Press, Cambridge, 2020).
[24] C. Pellegrini, R. Heid, and A. Sanna, J. Phys.: Mater. **5**, 024007 (2022).
[25] R. Akashi, K. Nakamura, R. Arita, and M. Imada, Phys. Rev. B **86**, 054513 (2012).
[26] F. Marsiglio, Phys. C (Amsterdam) **160**, 305 (1989).
[27] M. Rösner, S. Haas, and T. O. Wehling, Phys. Rev. B **90**, 245105 (2014).
[28] G. Schönhoff, M. Rösner, R. E. Groenewald, S. Haas, and T. O. Wehling, Phys. Rev. B **94**, 134504 (2016).
[29] E. R. Margine, H. Lambert, and F. Giustino, Sci. Rep. **6**, 21414 (2016).

[30] J. Bekaert, A. Aperis, B. Partoens, P. M. Oppeneer, and M. V. Milošević, Phys. Rev. B **96**, 094510 (2017).
[31] R. A. Jishi, D. M. Guzman, and H. M. Alyahyaei, Adv. Studies Theor. Phys. **5**, 703 (2011).
[32] C.-S. Lian, C. Si, and W. Duan, Nano Lett. **18**, 2924 (2018).
[33] F. Zheng and J. Feng, Phys. Rev. B **99**, 161119(R) (2019).
[34] J. Bekaert, M. Petrov, A. Aperis, P. Oppeneer, and M. V. Milošević, Phys. Rev. Lett. **123**, 077001 (2019).
[35] C.-S. Lian, C. Heil, X. Liu, C. Si, F. Giustino, and W. Duan, Phys. Rev. B **105**, L180505 (2022).
[36] S. Singh, A. H. Romero, J. D. Mella, V. Eremeev, E. Muñoz, A. N. Alexandrova, K. M. Rabe, D. Vanderbilt, and F. Muñoz, npj Quantum Mater. **7**, 37 (2022).
[37] C. Sevik, J. Bekaert, M. Petrov, and M. V. Milošević, Phys. Rev. Mater. **6**, 024803 (2022).
[38] S. He, J. He, W. Zhang, L. Zhao, D. Liu, X. Liu, D. Mou, Y.-B. Ou, Q.-Y. Wang, Z. Li, L. Wang, Y. Peng, Y. Liu, C. Chen, L. Yu, G. Liu, X. Dong, J. Zhang, C. Chen, Z. Xu *et al.*, Nat. Mater. **12**, 605 (2013).
[39] D. Liu, W. Zhang, D. Mou, J. He, Y.-B. Ou, Q.-Y. Wang, Z. Li, L. Wang, L. Zhao, S. He, Y. Peng, X. Liu, C. Chen, L. Yu, G. Liu, X. Dong, J. Zhang, C. Chen, Z. Xu, J. Hu *et al.*, Nat. Commun. **3**, 931 (2012).
[40] Q.-Y. Wang, Z. Li, W.-H. Zhang, Z.-C. Zhang, J.-S. Zhang, W. Li, H. Ding, Y.-B. Ou, P. Deng, K. Chang, J. Wen, C.-L. Song, K. He, J.-F. Jia, S.-H. Ji, Y.-Y. Wang, L.-L. Wang, X. Chen, X.-C. Ma, and Q.-K. Xue, Chin. Phys. Lett. **29**, 037402 (2012).
[41] N. Reyren, S. Thiel, A. D. Caviglia, L. F. Kourkoutis, G. Hammerl, C. Richter, C. W. Schneider, T. Kopp, A.-S. Rüetschi, D. Jaccard, M. Gabay, D. A. Muller, J.-M. Triscone, and J. Mannhart, Science **317**, 1196 (2007).
[42] Y. Guo, Y.-F. Zhang, X.-Y. Bao, T.-Z. Han, Z. Tang, L.-X. Zhang, W.-G. Zhu, E. G. Wang, Q. Niu, Z. Q. Qiu, J.-F. Jia, Z.-X. Zhao, and Q.-K. Xue, Science **306**, 1915 (2004).
[43] Y. in 't Veld, M. I. Katsnelson, A. J. Millis, and M. Rösner, Screening induced crossover between phonon- and plasmon-mediated pairing in layered superconductors, arXiv:2303.06220.
[44] J. Bardeen, L. N. Cooper, and J. R. Schrieffer, Phys. Rev. **108**, 1175 (1957).
[45] P. Coleman, *Introduction to Many-Body Physics* (Cambridge University Press, Cambridge, 2015).
[46] D. Costanzo, S. Jo, H. Berger, and A. F. Morpurgo, Nat. Nanotechnol. **11**, 339 (2016).
[47] D. Qiu, C. Gong, S. Wang, M. Zhang, C. Yang, X. Wang, and J. Xiong, Adv. Mater. **33**, 2006124 (2021).
[48] X. Xi, L. Zhao, Z. Wang, H. Berger, L. Forró, J. Shan, and K. F. Mak, Nat. Nanotechnol. **10**, 765 (2015).
[49] S. C. de la Barrera, M. R. Sinko, D. P. Gopalan, N. Sivadas, K. L. Seyler, K. Watanabe, T. Taniguchi, A. W. Tsen, X. Xu, D. Xiao, and B. M. Hunt, Nat. Commun. **9**, 1427 (2018).
[50] E. Khestanova, J. Birkbeck, M. Zhu, Y. Cao, G. L. Yu, D. Ghazaryan, J. Yin, H. Berger, L. Forró, T. Taniguchi, K. Watanabe, R. V. Gorbachev, A. Mishchenko, A. K. Geim, and I. V. Grigorieva, Nano Lett. **18**, 2623 (2018).
[51] A. Kamlapure, M. Simonato, E. Sierda, M. Steinbrecher, U. Kamber, E. J. Knol, P. Krogstrup, M. I. Katsnelson, M. Rösner, and A. A. Khajetoorians, Nat. Commun. **13**, 4452 (2022).
[52] L. Benfatto, C. Castellani, and T. Giamarchi, Phys. Rev. Lett. **98**, 117008 (2007).
[53] B. Chattopadhyay and S. R. Shenoy, Phys. Rev. Lett. **72**, 400 (1994).
[54] O. Parcollet, M. Ferrero, T. Ayral, H. Hafermann, I. Krivenko, L. Messio, and P. Seth, Comput. Phys. Commun. **196**, 398 (2015).
[55] N. Wentzell, H. U. Strand, S. Kaeser, D. Simon, A. Hampel, E. G. C. P. van Loon, O. Parcollet, D. Philipp, and M. Zingl, TRIQS/tprf: Version 3.1.1 (2022), doi: 10.5281/zenodo.6335758.